NEUTRINO PROPERTIES

Klaus Winter
CERN, Geneva, Switzerland

ABSTRACT

A picture of the properties of neutrinos, as determined from particle physics experiments, is given, including the questions of mass, of Dirac or Majorana states, of how many flavour states exist, of the electric charge and charge radius, of the magnetic moment and of lepton number conservation.

1. INTRODUCTION

In a letter [1] addressed to the "dear radioactive ladies and gentlemen", written in December 1930, Wolfgang Pauli proposed, as a "desperate remedy" to save the principle of conservation of energy in beta-decay, the idea of the neutrino, a neutral particle of spin $^1/_2$ and with a mass not larger than 0.01 proton mass. "The continuous beta-spectrum [2] would then become understandable by the assumption that in beta-decay a neutrino is emitted together with the electron, in such a way that the sum of the energies of neutrino and electron is constant."

Pauli did not specify at that time whether the neutrino was to be ejected or created. In his famous paper "An attempt of a theory of beta-decay" [3] E. Fermi used the neutrino concept of Pauli together with the concept of the nucleus of Heisenberg. He assumed that in the beta-decay a pair of electron and neutrino is created, analogous to photons in transitions between nuclear states. This theory accounted successfully for the observed continuous electron spectrum in beta-decay. Near the end point Fermi found closest ressemblance with data for a neutrino mass of zero, in agreement with a previous observation of F. Perrin [4].

Our present view is that in our world neutrinos have no SU(3) x U(1) quantum numbers like colour or electric charge, and, hence, that they decouple in the infrared limit [5]. We see neutrinos of these properties as a kind of platonic dream of the elementary particle.

For cosmologists and for us at this symposium, the idea of a universe filled with relic neutrinos from the big-bang is a consequence. Relic neutrinos are thought to outnumber the neutrons, protons and electrons of ordinary matter by about 10^{10}. On the average every cubic centimeter in the universe contains some 450 of them. Supposedly massless they are capable of passing through the sun and the earth as if they were not there.

However, if they had non-zero rest mass they could slow down and come to rest, become gravitationally bound in galaxies or clusters of galaxies, and thereby participate in their evolution and may close the universe [6].

This lecture attempts to give a new picture of the properties of neutrinos, as determined from particle physics experiments, of the number of different flavours they may have, of their electric charge and magnetic moment, and of their mass and of the conservation laws they are subject to.

2. NUMBER OF NEUTRINO FLAVOURS

It is one of the most puzzling experimental facts of particle physics that matter has been found existing in replicates, or families, of which we know three today, each with a charged lepton and a neutrino. The family or flavour number of the leptons is found to be conserved, although we would not be surprised to find inter-flavour mixing for leptons in the same way as for quarks.

How many such families exist in nature? This fundamental question has found answers, from laboratory experiments and from astrophysical constraints. The well-known astrophysical constraint, derived from the observations of primordial D, He^3, He^4, and ^7Li applies to very light neutrinos only; the classical calculation [7] permitted at the most only one new family.

$$\Delta N_\nu = (N_\nu - 3) < 1 \ . \tag{1}$$

A reappraisal [8] of this bound, in view of uncertainties in the neutron half-life, systematic errors in the abundance of He^4 and new data suggesting destruction of He^3 in stars, tends to increase the cosmological upper bound on N_ν to

$$\Delta N_\nu = (N_\nu - 3) < 2.5 \ . \tag{2}$$

Recent UA1 and UA2 data from the CERN $p\bar{p}$ collider [9] suggest that (90% c.l.)

$$\Delta N_\nu < 2.4 \pm 1.0 \ , \tag{3}$$

where the error reflects theoretical uncertainties. This bound is derived from the measurement of the ratio

$$R = \frac{\sigma(p\bar{p} \to Z(\to e^+e^-)X)}{\sigma(p\bar{p} \to W(\to e\nu)X)} = 0.108 \begin{matrix} +\ 0.025 \\ -\ 0.033 \end{matrix} \ (\text{UA1}) \ 0.136 \begin{matrix} +\ 0.041 \\ -\ 0.033 \end{matrix} \ (\text{UA2})$$

which can be expressed in terms of three factors

$$R = \frac{\sigma(p\bar{p} \to ZX)}{\sigma(p\bar{p} \to WX)} \cdot \left(\frac{\Gamma(W \to \text{all})}{\Gamma(W \to e\nu)} \right) \left(\frac{\Gamma(Z \to e^+e^-)}{\Gamma(Z \to \text{all})} \right) .$$

The first one can be calculated from QCD giving 0.30 ± 0.02; $\Gamma(W \to e\nu)$, $\Gamma(W \to \text{all})$ and $\Gamma(Z \to e^+e^-)$ are directly calculated from the standard model, and hence $\Gamma(Z \to \text{all})$ follows from the measurement of R. The total width of the Z^0 is related to the number of fermion doublets for which the decay $Z^0 \to f\bar{f}$ is kinematically allowed. Assuming that for any additional fermion family only the neutrino is less massive than $M_Z/2$ we can determine the upper bound on the number of neutrino flavours with $M_\nu < M_Z/2$ given in eq. (3). The near equality with the astrophysical bound leaves little space for the contribution of massive neutrinos.

In the near future we expect more accurate measurements at the large e^+e^- colliders SLC and LEP which will permit "counting" the number of neutrino flavours.

The cross section of radiative Z^0 production with Z^0 decaying into $\nu\bar{\nu}$

$$e^+e^- \to Z^0\,\gamma, \quad Z^0 \to \nu\bar{\nu}$$

is proportional to N_ν; hence, an additional neutrino flavour will increase its value by 30% and a 5% measurement [10] will determine $\Delta N_\nu = 1$ with five standard deviations.

The total width of the Z^0 is expected to be $\Gamma_{TOT}(Z^0) = 2.78$ GeV for decays into three families of fermions and assuming $\sin^2\theta_W = 0.23$. One additional neutrino flavour will increase this width by

$$\Delta\Gamma_{TOT}(\Delta N_\nu = 1) = 170 \text{ MeV} \ . \tag{4}$$

Making use of the excellent energy definition of the LEP beams the total width may be determined [10] with an error of 20 MeV, and $\Delta N_\nu = 1$ with 8σ.

3. DO NEUTRINOS HAVE NON-ZERO MASS?

Neutrinos may be described by a conventional Dirac field associated with an ordinary mass parameter or by a Majorana field. If the lepton flavour number were not conserved, neutrinos would have to be described by a superposition of Dirac fields, associated with new phenomena such as neutrino oscillations, neutrino decays and neutrino-less double β-decay.

Are neutrinos Dirac or Majorana particles? To answer this question let us investigate how they would transform under CPT [11]. Suppose there exists a massive neutrino ν_- with negative helicity; CPT transforms it into the antineutrino with positive helicity $\bar{\nu}_+$ (see figure 1). Being massive ν_- travels slower than light. An observer travelling faster can overtake it. In its frame the neutrino travels in the opposite direction while spinning the same way as in the original frame. Hence, by Lorentz transformation ν_- can be turned into ν_+. This state may or may not be the same as the CPT image of ν_-.

Suppose it is not the same state (fig. 1a). Then it has its own CPT image, $\bar{\nu}_-$ Altogether there are four states with a common mass parameter, which are described by a Dirac field. A massive Dirac neutrino has a (Pauli) magnetic dipole moment, and perhaps an electric dipole moment. Thus, in the Dirac field case, the state ν_- can also be converted into its positive helicity partner ν_+ by an external magnetic or electric field.

In the second case, depicted in Figure 1(b), the positive helicity state obtained by Lorentz transformation is the same as the CPT mirror-image of ν_-. This two-state neutrino is described by a Majorana field. A Majorana neutrino being its own antiparticle clearly carries no lepton number and will therefore lead to lepton number violation.

If neutrinos have zero mass there is no distinction possible between a Dirac and a Majorana neutrino [12]. Two Dirac states ($\bar{\nu}_-$, ν_+) need not exist in nature [13] and there would just be two states (ν_-, $\bar{\nu}_+$), and it becomes purely a matter of semantics whether one chooses to call them a Dirac neutrino and its antiparticle, or the two helicity states of a Majorana neutrino.

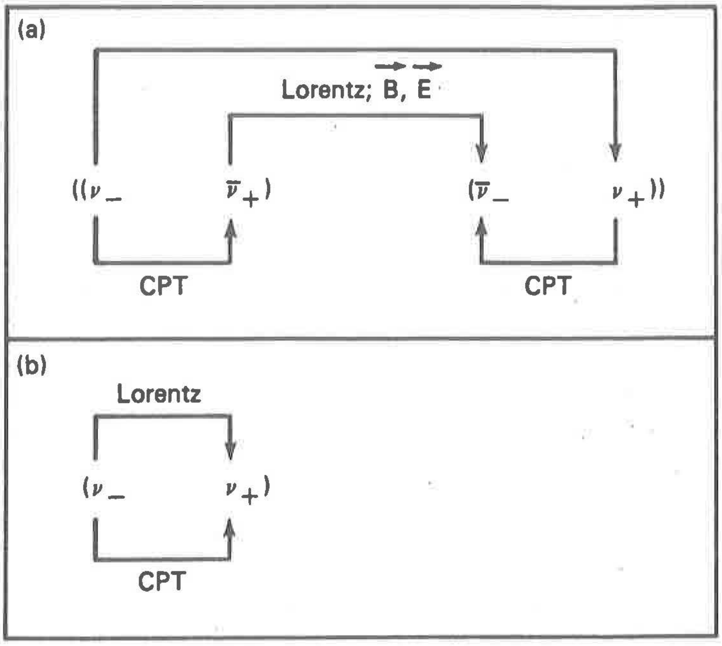

Fig. 1 (a) The four states of a massive Dirac neutrino; (b) The two states of a Majorana neutrino

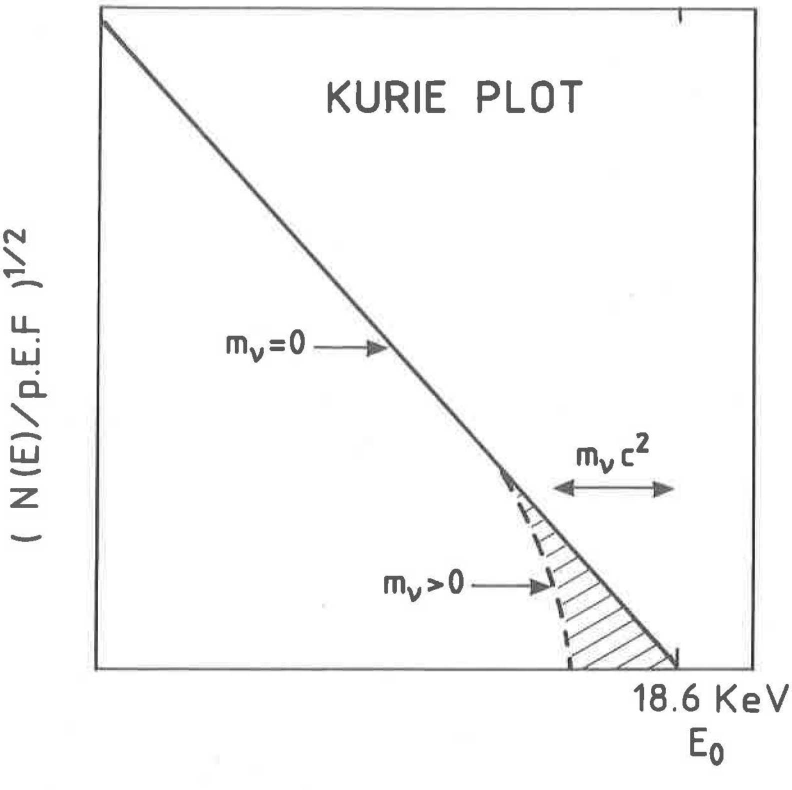

Fig. 2 Kurie plot of $^{3}H \rightarrow {}^{3}He + e^{-} + \bar{\nu}_e$ beta-decay and the effect of non-zero neutrino mass

There is only one experimental approach which would allow massive Dirac neutrinos to be distinguished from massive Majorana neutrinos: neutrino-less double-beta decay. The present status of searching for this process is reviewed in Chapter III.4.

If lepton flavour number is not conserved in nature we expect neutrinos to mix, in analogy to quarks. The flavour eigenstates $\alpha(e,\mu,\tau)$ will then be described by a superposition of Dirac mass eigenstates $i(1,2,3)$

$$|\nu_\alpha> = \Sigma_i U_{\alpha i} |\nu_i> \quad (5)$$

where the mixing parameters $U_{\alpha i}$ form a unitary mixing matrix analogous to the Kobajashi-Maskawa matrix of quark mixing, with a host of conceivably associated new phenomena, which extend the sensitivity to mass parameters as small as 10^{-6} eV.

There are currently four claims of evidence of finite neutrino mass in the literature. Three of them are at present contradicted by new measurements and subject to criticism. In one case, however, the solar neutrino puzzle, the experimental evidence has not been contradicted and a new possible explanation in terms of neutrino oscillations has been proposed. The present situation will be described in the following Chapters: direct measurements of mass parameters by kinematics (III.1), neutrino mixing (oscillations and decays) (III.2), the solar neutrino puzzle (III.3) and search for neutrino-less double beta-decays (III.4).

3.1 Direct Neutrino Mass Measurements by Kinematics

Direct mass measurements on all three neutrino flavours have been performed. The most precise results are summarized in table 1; the methods have recently been described in an excellent review by K. Bergkvist [14].
Note the claims of non-zero mass of $\bar{\nu}_e$ deduced from a series of measurements of the beta-spectrum of tritium near the end point by the ITEP group [15] and from a measurement at low energy by Simpson [16]. In the following we discuss new experimental data contradicting them and criticisms aiming at explaining the claimed non-zero results by conventional arguments which may have been neglected by the authors.

Table 1

Summary of direct measurements of neutrino masses

Neutrino	Method	Group	Result
$\bar{\nu}_e$	^3H decay	ITEP (15)	$m_{\nu_e} = 31.3 \pm 0.3$ eV
	^3H decay	Simpson (16)	$m_{\nu_e} = 17$ KeV
			$\lvert U_{ei}\rvert^2 = 0.3$
ν_μ	$\pi \to \mu\nu_\mu$ at rest	SIN (17)	$m_{\nu_\mu} < 270$ KeV
ν_τ	$\tau \to 6\pi\nu_\tau$	ARGUS (18)	$m_{\nu_\tau} < 56$ MeV

Figure 2 shows schematically the effect of a non-zero neutrino mass on the shape of the beta spectrum in a Fermi-Kurie plot for $^3H \to {}^3He + e^- + \bar{\nu}_e$. How well can the shaded area between the two cases shown, $m_\nu = 0$ and $m_\nu \neq 0$, be measured? Integrating the beta spectra in an interval ΔE from the end point we find a ratio of areas for the two cases

$$R = \frac{A(m_\nu)}{A(0)} = (1 - (\frac{m_\nu c^2}{\Delta E})^2)^{3/2} \qquad (6)$$

and, hence, the sensitivity to non-zero neutrino mass proportional to m_ν^3. Assuming a spectrometer resolution of 10 eV, the number of events has to be increased by a factor of ~ 15 to improve the sensitivity from $m_\nu = 10$ eV to $m_\nu = 5$ eV. This requirement of high statistics in the measurement of the tritium beta-decay spectrum near the end point is one of the 3 basic experimental problems encountered:

1. The counting rate in an interval of $\Delta E = 25$ eV from the end point E_0 is a fraction of only $3 \cdot 10^{-9}$ of the total tritium decay rate. As the sources have to be thin to keep the energy loss small the required rates have to be achieved by preparing sources of large area.

2. The thickness profile of the source has to be accurately known to correct for the energy loss, and the spectrometer has to provide adequate resolution (~ 20 eV) for large area sources.

3. The final state spectrum of ^3He is affected by the preparation of the sources. By choosing suitable substrates for implanting tritium atoms one can calculate the binding energy of the tritium atoms and molecules

in the substrate reliably and hence predict the ^{3}He final state spectrum.

The ITEP group [15], claiming evidence for a non-zero mass of the electron antineutrino (see Table 1), has made important improvements in sensitivity to m_ν as compared with earlier measurements by K.E. Bergkvist [19]. They developed a new magnetic spectrometer (Tretyakov [20]) with high dispersion and low background, modern counting techniques and sources of higher specific (activity per cm^2) activity. However, their claim has been subject to some criticism, on the way the ^{3}He final state spectrum has been accounted for [21], and on the evaluation of the effective resolution function of the spectrometer [22]. But up to now no other experiment has reached comparable sensitivity to give an independent result which would either confirm or invalidate their result.

Very recently a group from the University of Zürich led by W. Kündig, reported [23] a new measurement of the end point region of the tritium beta-decay spectrum.

They used a toroidal field spectrometer of the Tretyakov type [20] shown schematically in figure 3. A good impression of the size and complexity of this instrument can be obtained from the photography on fig. 4. The source assembly consists of 10 rings, each with 10 cm diameter and 1 cm width, providing a total source surface of 157 cm^2. An electrostatic retarding field around the source decelerates electrons to 2.2 KeV. The source length is compensated by a gradient voltage, proportional to the spectrometer dispersion, applied along the rings. Spectra are recorded by stepping the retarding voltage while keeping the magnetic field constant for focussing 2.2 KeV electrons. At the exit of the spectrometer, electrons are accelerated again by a voltage of 15 KV and enter the position sensitive detector.

This spectrometer has a resolution of 27 eV (FWHM), calculated by Monte Carlo simulation (see curve SR in figure 5). The sources were prepared by implanting tritium ions into carbon, evaporated onto aluminium backing foils. The depth profile of the tritium concentration was measured using a nuclear recoil technique. The resulting energy loss distribution (EL) was then calculated and is shown alone and folded with the spectrometer resolution in figure 5. This method of determining the source thickness directly instead of invoking it from conversion electron measurements [15] is one of the factors which contribute to the reliability of this new result. The intensity of back scattering from the source was treated as a free parameter in the data analysis.

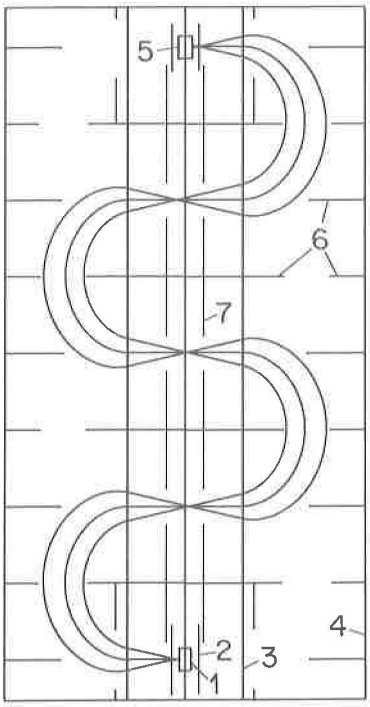

Fig. 3 Schematic view of the spectrometer of the Zürich group. The source (1), deceleration electrode (2), detector (5), baffles (6) (7) [23].

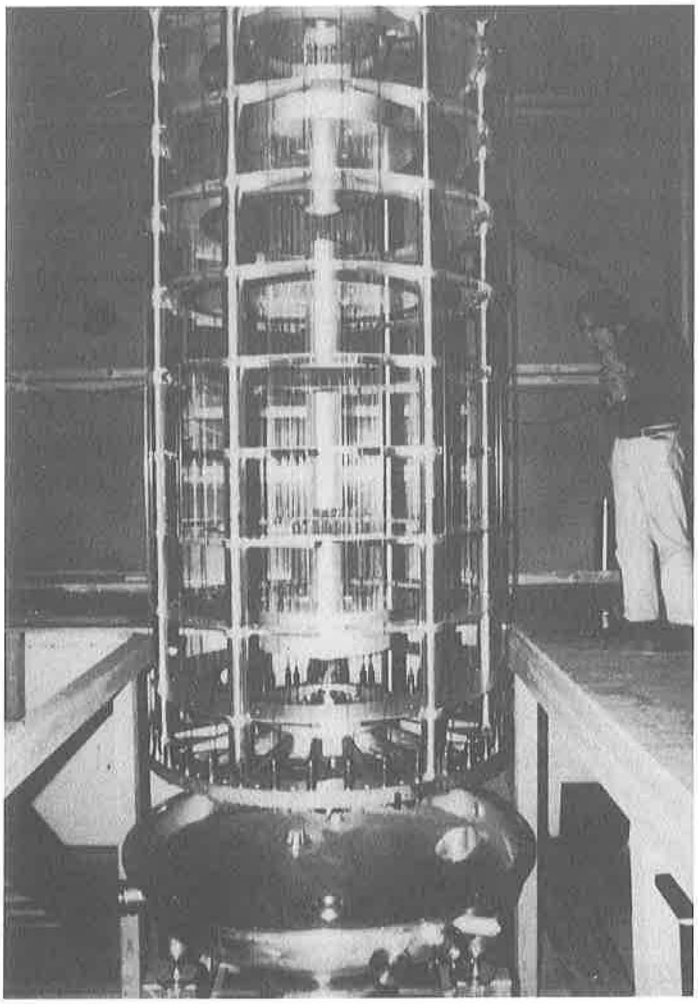

Fig. 4 The beta spectrometer of the Zürich group.

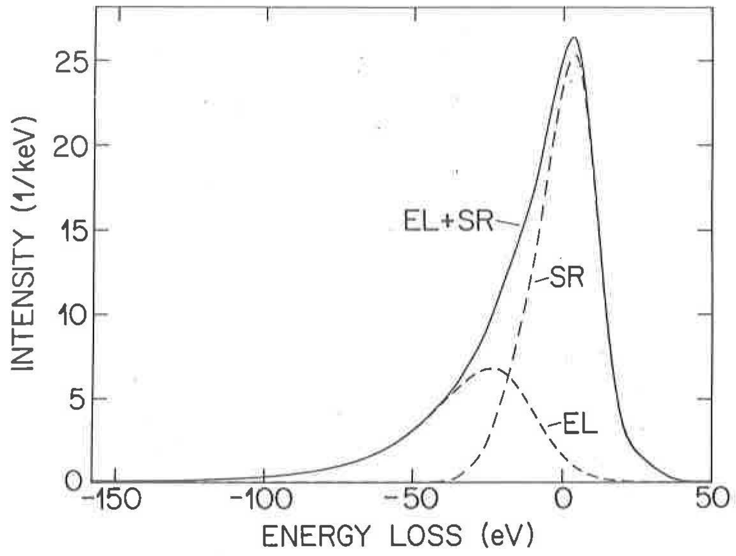

Fig. 5 The resolution function of the Zürich detector composed of the spectrometer resolution (SR) and the energy loss (EL).

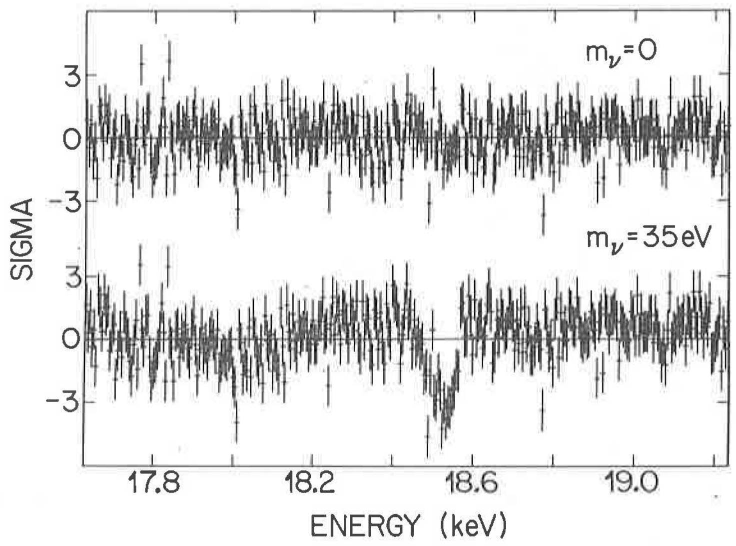

Fig. 6 Deviation of the measurements of the Zürich group from the expected distributions for $m_\nu = 0$ and $m_\nu = 35$ eV.

Figure 6 shows a section of the spectra near the end point compared with the shape expected for the values of $m_\nu = 0$ and $m_\nu = 35$ eV claimed by the ITEP group [15]. The result of the fitting procedure of m_ν^2 by minimizing χ^2 and varying all other parameters is shown in figure 7. The result obviously depends on the electronic final state spectrum assumed. The CH_3T case was used to represent the carbon-tritium molecular bonds. A statistical 95% confidence upper limit of $m_\nu^2 < 106$ eV^2 is established. Adding linearly a systematic error estimate of $m_\nu^2 < 204$ eV^2, the authors arrived at an upper bound of

$$m_\nu < 18 \text{ eV} \quad (95\% \text{ c.l.}) \tag{7}$$

and conclude that they find no evidence for a non-zero mass for the electron antineutrino, in strong contradiction to the claim of the ITEP group [15]. Further measurements of this group may improve the sensitivity to a 95% confidence limit of 10 eV, allowing a neutrino mass of 18 eV to be established with three standard deviations

Based on measurements of the low energy part of the tritium beta spectra performed in a Si(Li) detector implanted with tritium, J.J. Simpson [16] has reported evidence for a distortion in the Kurie plot (see figure 8) starting below a kinetic energy of 1.5 KeV, 17.1 KeV below the end point, which he claims is due to a heavy neutrino of $m_\nu = (17.1 \pm 0.2)$ KeV with a mixing parameter of $|U_{ei}|^2 = 0.03$. Several groups [24-28] have published measurements on the beta spectrum of ^{35}S where the effect of a 17 KeV neutrino would show up at 150 KeV.

No such distortions have been observed and upper limits for the mixing parameter are reported which are much smaller than the effect claimed. For example, Ohi et al [25] report $|U_{ei}|^2 < 0.2\%$, consistent with zero mixing (see figure 9). Simpson has shown recently [29] that the data analysis performed in references [24-26] has overestimated the sensitivity, leaving however without valid objection, the negative evidence reported in references [27] and [28]. More recently, Lindhard and Hansen [30] have shown that the distortion observed by Simpson can be explained conventionally by properly taking account of Coulomb screening effects and chemical binding energy in calculating the lower end of the tritium beta spectrum (see fig. 10).

Based on the negative experimental evidence in ^{35}S [27,28] and the conventional explanation of the distortion [30], we feel entitled to dismiss the 17 KeV neutrino claim.

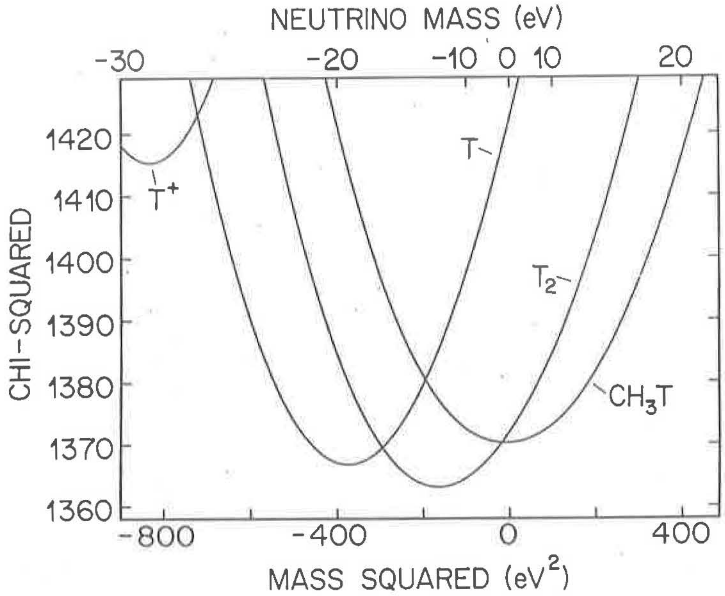

Fig. 7 Chi-square distributions of the fits as a function of m_ν^2 for different models of tritium binding in carbon. The preferred model is CH T. [23].

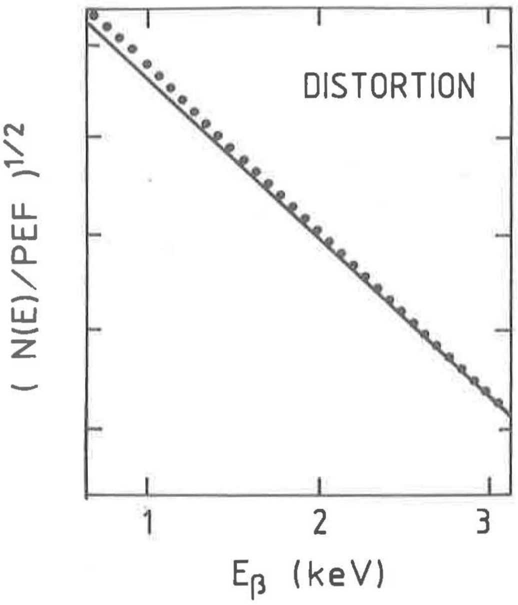

Fig. 8 Distortion of the Kurie plot of tritium beta decay at the low energy end as observed by Simpson [21].

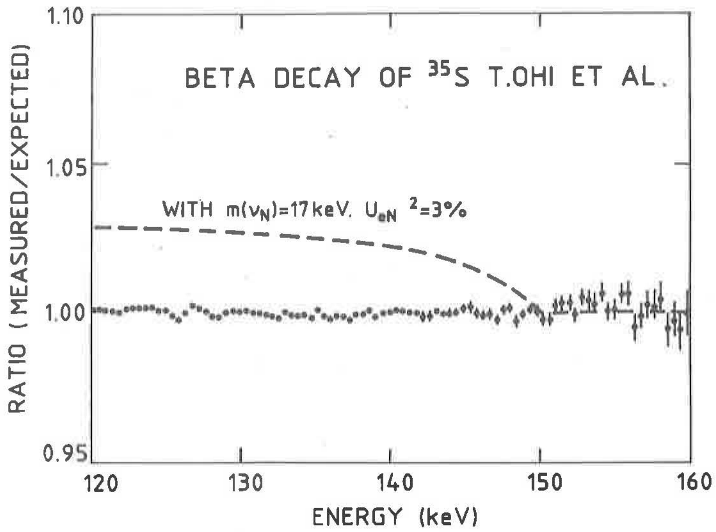

Fig. 9 Beta spectrum of ^{35}S as measured by Ohi et al. [25] and deviation expected for a 17 keV neutrino. See, however, ref. [29] for comments on the analysis.

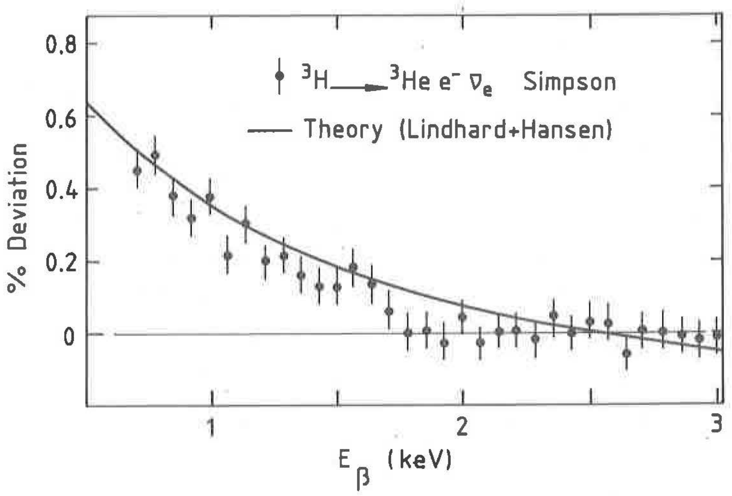

Fig. 10 Deviation of Simpson's measurement [21] and an improved calculation of the beta spectrum [30] without a 17 keV neutrino.

3.2 Neutrino mixing

If Dirac mass eigenstates (i = 1,2,3) exist, they need not coincide with the weak flavour $\alpha = (\nu_e, \nu_\mu, \nu_\tau)$ eigenstates but rather with a linear combination (see eq.(5)) thereof,

$$|\nu_\alpha > = \Sigma_i U_{\alpha i} | \nu_i > ,$$

where $U_{\alpha i}$ are the elements of a unitary mixing matrix. A pure flavour state $|\nu_\alpha >$, created at time zero in a weak decay process also involving a charged lepton of the same flavour, may, by mixing, evolve with time into another state with a different flavour β

$$|\nu(t)> = \Sigma_i U_{\alpha i} U^*_{\beta i} e^{-iEit} |\nu_\beta> . \tag{8}$$

The physical processes of neutrino oscillations, allowed by eqs.(5) and (8),

$$\begin{array}{c} \nu_\alpha \leftrightarrow \nu_\beta \\ \bar{\nu}_\alpha \leftrightarrow \bar{\nu}_\beta \end{array} \tag{9}$$

are closely related if CP invariance holds for these lepton flavour violating processes.

Transitions between neutrinos and antineutrinos of different flavours

$$\nu_\alpha \leftrightarrow \bar{\nu}_\beta \tag{10}$$

may also occur and would have to change the helicity; helicity flip amplitudes being proportional to m_ν / E_ν, these transitions would therefore be expected to be much weaker. Experimental results are expressed in terms of upper limits on $|U_{\alpha i}|^2$ as functions of the mass parameters m_i. The simplifying assumption of a two-state system is generally made and the results are given in terms of $\Delta m^2 = |m^2{}_1 - m^2{}_2|$ (in units of eV^2) and $\sin^2 2\theta$. The experimental limits quoted in this way in the literature can easily be extended to a three-state system [31]. The probability of appearance of a new flavour state thus depends on four parameters, according to the following expression derived from eq.(8)

$$P_{\alpha\beta}(E_\nu, L, \Delta m^2, \theta) = \sin^2 2\theta \times \sin(1.27 \cdot \Delta m^2 \, L/E_\nu), \tag{11}$$

where E_ν is the neutrino energy (in MeV), L the distance from the creation of the flavour state α (in m). After an oscillation length of

$$L_0 = \pi/2 \; E_\nu/1.27 \cdot \Delta m^2$$

$P_{\alpha\beta}$ passes through a maximum. The probability of disappearance of the flavour α is related to $P_{\alpha\beta}$ by unitarity

$$P_{\alpha\alpha} = 1-P_{\alpha\beta} \; . \tag{12}$$

Table 2 summarizes for the three most abundant sources of neutrinos the initial flavour, the mean neutrino energy or the energy range, the distances L used up to now for experiments and the squared mass difference, Δm^2, to which these experiments are sensitive. The transition probabilities for flavour disappearance experiments, $P(\nu_\alpha \rightarrow \nu_\alpha)$, and for new flavour appearance experiments, $P(\nu_\alpha \rightarrow \nu_\beta)$, are shown in figure 11. The amplitude of the oscillation is given in both cases by $\sin^2 2\theta$, the mixing parameter, and the frequency by $\Delta m^2 \cdot L/E$. For large values of $L/E >> 1/\Delta m^2$ the frequency of oscillations is very large and experiments will average over them, because of the extended dimensions of the source and the detector. In the disappearance case the mean transition probability in this situation becomes

$$P_{\alpha\alpha}(L/E >> 1/\Delta m^2) = 1 - {}^1/_2 \sin^2 2\theta \; ,$$

and in the new flavour appearance case it becomes

$$P_{\alpha\beta}(L/E >> 1/\Delta m^2) = {}^1/_2 \sin^2 2\theta \; .$$

Obviously, it is experimentally easier to detect small mixing parameters in "appearance" experiments than in disappearance experiments.

Table 2

Summary of the most abundant neutrino sources

Source	Flavour	$\bar{E}_\nu$	L_{max}	Δm^2
Nuclear reactor	$\bar{\nu}_e$	3 MeV	100 m	0.03 eV^2
Accelerators	ν_μ	0.035-100 GeV	1000 m	0.03-100 eV^2
Sun	ν_e	1-10 MeV	10^{11} m	10^{-11} eV^2

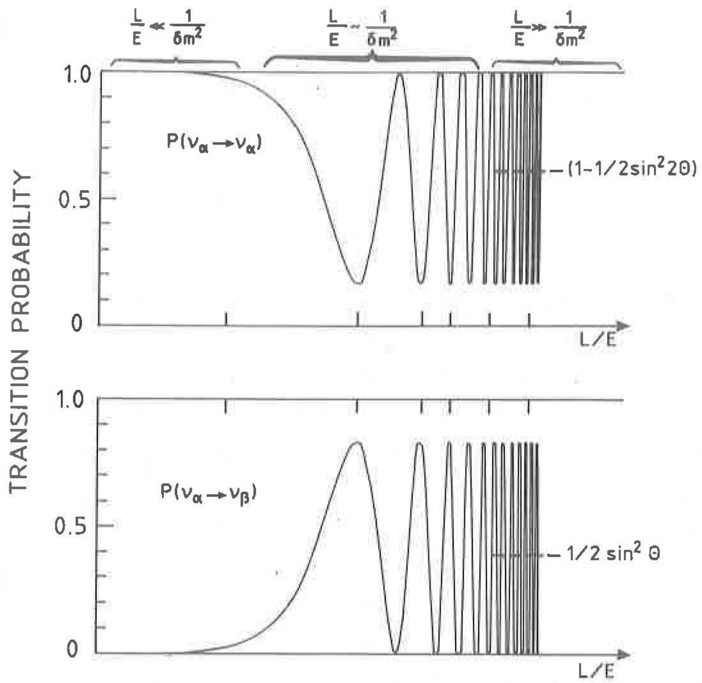

Fig. 11 The two types of neutrino oscillation experiments; disappearance of flavour α and appearance of a new flavour β.

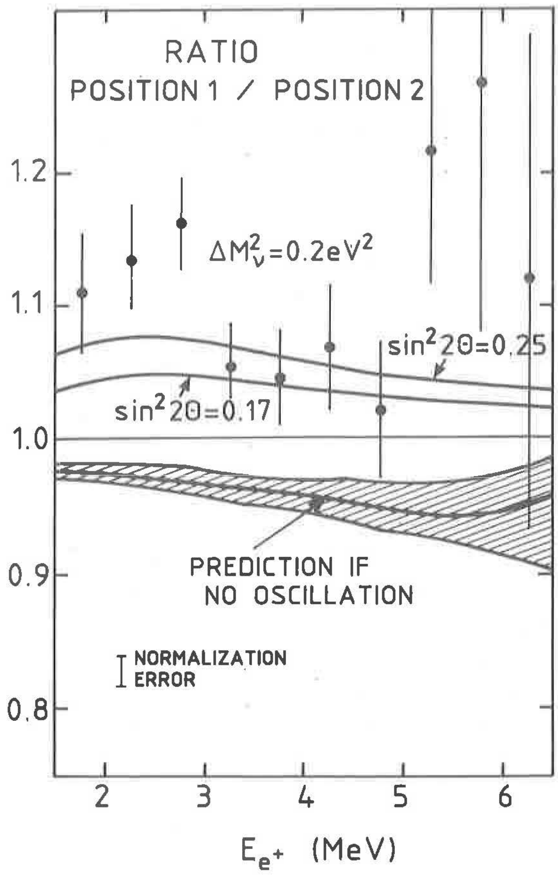

Fig. 12 Ratio of results of the Bugey experiment [34] at position 1 and position 2 as a function of positron energy. Shown are expectations with and without neutrino oscillation.

Electron antineutrinos from nuclear reactors have energies below the threshold for the charged current reactions of muon- and tau-flavour. These sources can therefore only be used for disappearance experiments and are not sensitive to very small values of $\sin^2 2\theta$ but to small $\Delta m^2 \sim 0.02$ (eV^2). Accelerators are abundant sources of high energy muon-neutrino beams which can be used for appearance experiments; however, because of the higher energies involved, they are sensitive to rather larger values of $\Delta m^2 \sim 1\text{-}100\ eV^2$; because of the small background they are sensitive to small mixing parameters, $\sin^2 2\theta \sim 10^{-3}$. Solar neutrinos provide the unique opportunity for particle physics to explore very small mass differences, $\Delta m^2 \sim 10^{-11}\ eV^2$.

Neutrino oscillation experiments of the disappearance type have been performed using nuclear power reactors with 60 to 2800 MW thermal power at distances ranging from 8.7 m to 64.7 m from the core (see table 3).

Table 3

Parameters of disappearance type neutrino oscillation experiments at nuclear power reactors

Reactor	Reference	Power (MW)	Distances (m)	Statistics
Ill (F)	[32]	57	8.7	10^4
Gösgen (CH)	[33]	2800	37.9, 45.9, 64.7	10^4
Bugey (F)	[34]	2800	13.6, 18.3	$2\text{-}4 \cdot 10^4$
Savannah River (USA)	[35]	2300	18.2, 23.8	$2 \cdot 10^4$
Rovno (SU)	[36]	1375	18	$1.5 \cdot 10^4$

The reaction $\bar{\nu}_e p \rightarrow e^+ n$ is measured by detecting the recoil neutron and measuring the energy of the positron which is related to the neutrino energy by the relation $E_\nu = E_e + 1.8$ MeV.

Comparing the event rates and the spectra at two distances the Grenoble-Annecy group working at the Bugey reactor [34] has claimed evidence for neutrino oscillations with $\Delta m^2 = 0.2\ eV^2$ and $\sin^2 2\theta = 0.25$. The observed ratio of rates at the two distances (see table 3) is shown as a function of the positron energy in figure 12 and compared with the ratio expected without oscillation. The ratio of the observed and expected rates is

$$R = N(\text{close det})/N(\text{far det}) = 1.102 \pm 0.014(\text{stat.}) \pm 0.028(\text{syst.})$$

The experimental points in figure 12, however, do not follow the trend expected for neutrino oscillation which is also shown. The other experiments mentioned in table 3 do not find evidence for the oscillation effect claimed. The combined ILL and Gösgen experiments contradict the claim [33].

Analysing the Bugey experiment more closely Zacek et al. [33] noted that the spectrum observed at distance 1 agrees well with a spectrum calculated assuming no oscillation (see figure 13a) whereas the spectrum predicted for the claimed oscillation parameters shows a marked discrepancy at low energies (see figure 13b). The measurement at distance 2 has been incriminated as it shows a discrepancy in both cases (see figure 13c and d). The spectra measured at Gösgen by the Caltech-SIN-TUM group shows good agreement with the Bugey 1 spectrum assuming no oscillation and strongly disagrees with the prediction for the claimed oscillation parameters (see figure 14). The Bugey effect is shown (95% confidence area) shaded in figure 15 together with the limits derived from the other experiments. The regions to the right of the curves shown are excluded. The dotted curve labelled Gösgen [33] which uses measurements at all three distances and at ILL and the neutrino spectrum determined separately, strongly invalidates the Bugey claim.

More restrictive new limits for $\nu_\mu \to \nu_e$ oscillations have been reported by several groups which searched for ν_e interactions in bubble chambers, at BNL [37] and in BEBC at CERN [38] and in electronic detectors, at BNL [39] and by the CHARM Collaboration at CERN [40]. The Bugey claim and the Gösgen limit are also shown. Present limits from $\nu_\mu \to \nu_x$ disappearance and $\nu_\mu \to \nu_\tau$ appearance experiments are summarized in figures 17 and 18. Also shown (dotted) are limits which can be expected in the near future from experiments which have been proposed or discussed. The most sensitive limits in terms of Δm^2 either use very massive detectors (GRANSASSO, under construction for proton decay search) at large distances from the CERN SPS or high intensity sources of low energy ν_μ beams from pion decay at rest (LAMPF E645 SNS). The former could compete with further measurements at nuclear power reactors and decrease the upper limit on Δm^2 to 0.002 eV^2, while the latter could decrease the limit on $\sin^2 2\theta$ to 10^{-3}.

If the eigenstates in eq.(5) have large enough mass differences neutrino decays may occur [41] either by charged-current interaction

$$\begin{aligned} \nu_i &\to e^- e^+ \nu_e, \quad \mu^- e^+ \nu_e \\ \nu_i &\to \mu^- \mu^+ \nu_\mu, \quad e^- \mu^+ \nu_\mu , \end{aligned} \tag{13}$$

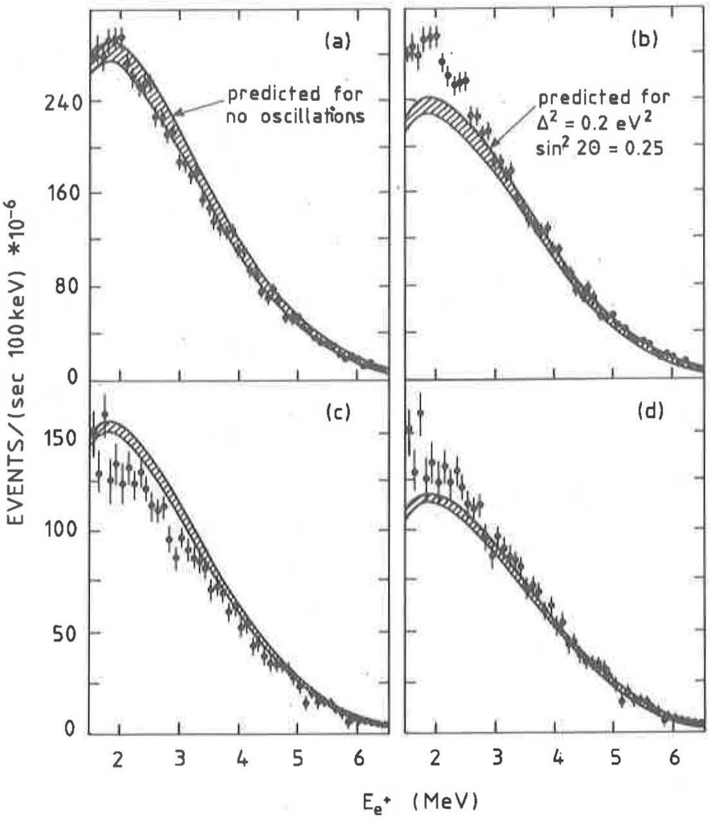

Fig. 13 Positron spectra observed at the two positions in the Bugey experiment. Prediction for no oscillation (a) in position I, (c) in position II; prediction for neutrino oscillation (b) in position I, (d) in position II.

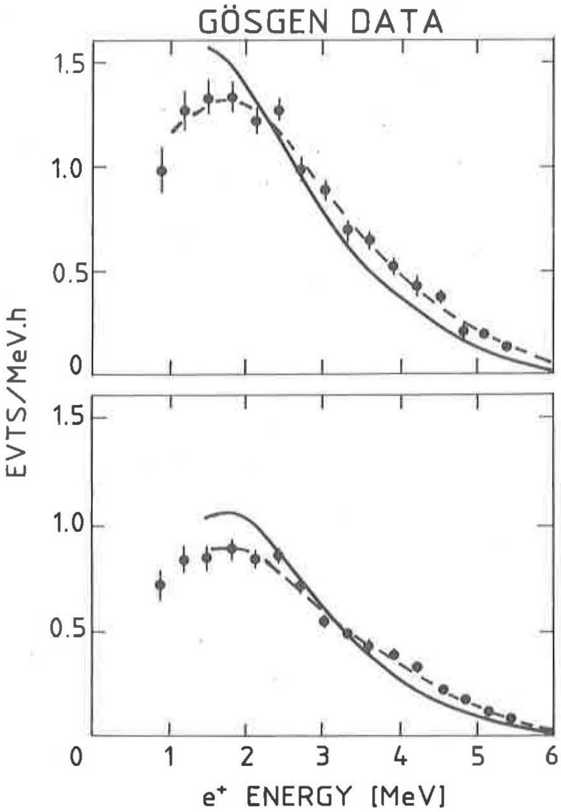

Fig. 14 Positron spectra measured in the Gösgen experiment [33] and compared with the Bugey I spectra, broken line no oscillation, full line for oscillation. Upper figure for Gösgen position 1, lower for Gösgen position 2.

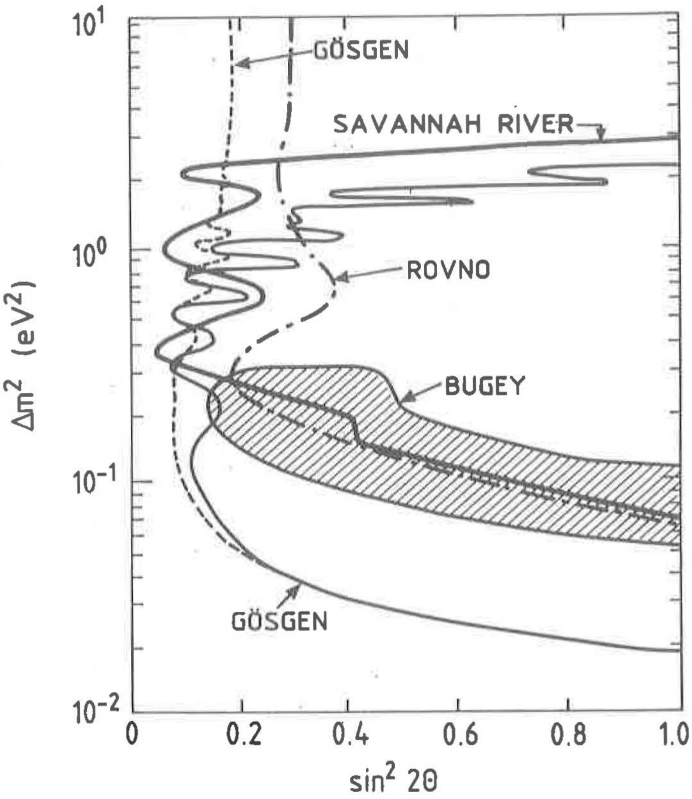

Fig. 15 Summary of limits from neutrino disappearance experiments at nuclear reactors. The area to the right side of the curves are excluded at the 90% c.l., the shaded area shows the Bugey [34] claim for oscillations.

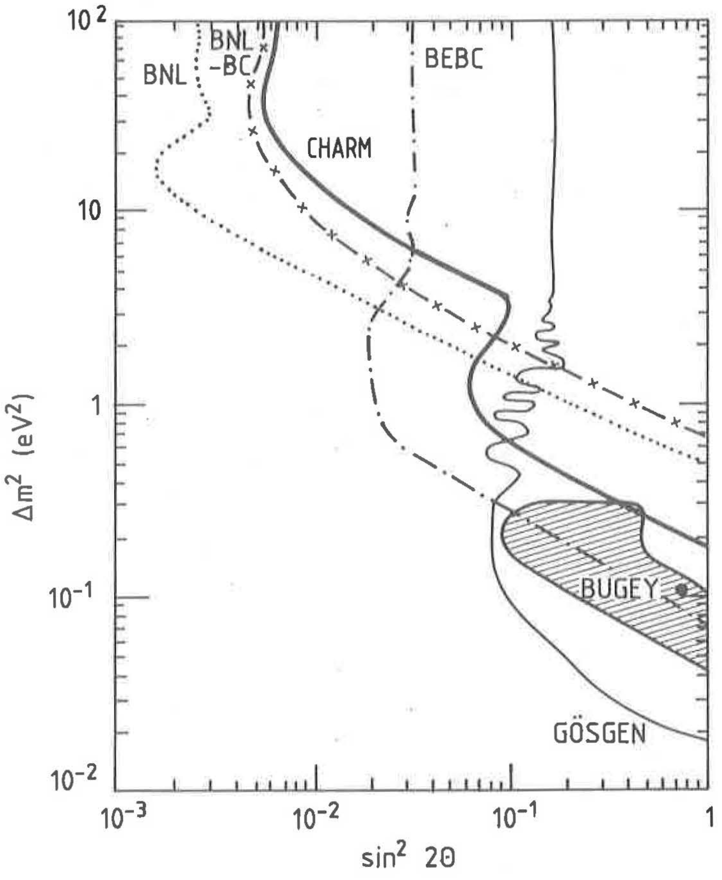

Fig. 16 Summary of 90% confidence limits from $\nu_\mu \rightarrow \nu_e$ appearance experiments at accelerators.

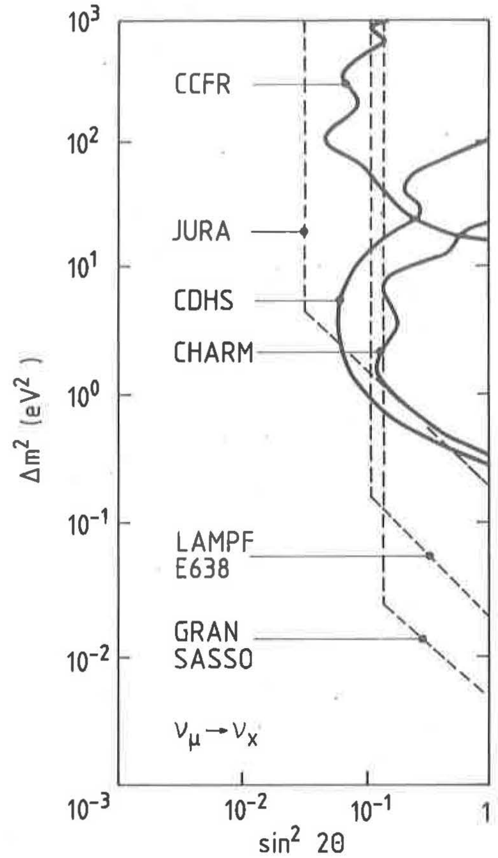

Fig. 17 Summary of limits on $\nu_\mu \to \nu_x$ disappearance experiments and expected sensitivity of proposed future experiments (dotted lines).

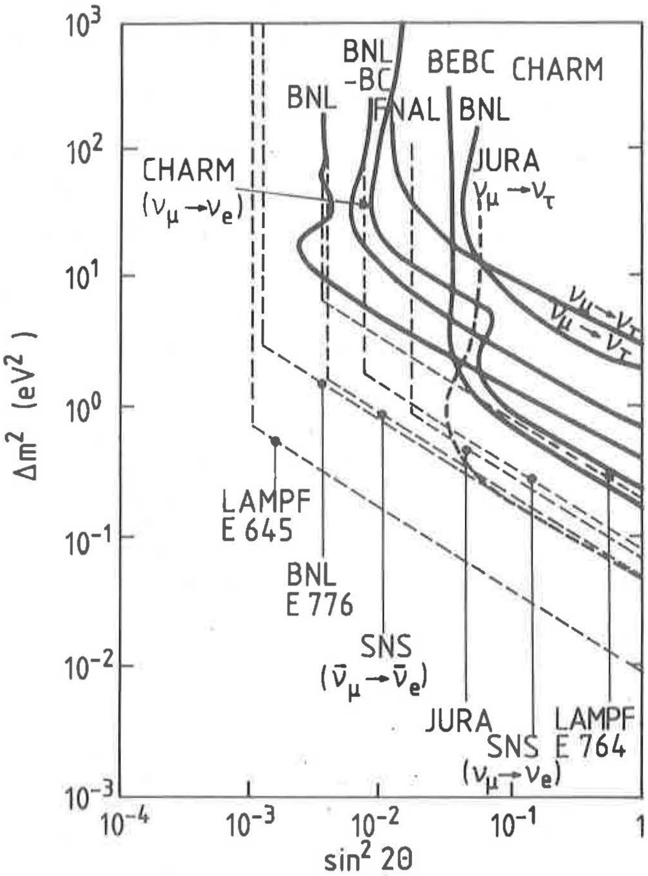

Fig. 18 Results of various appearance experiments, $\nu_\mu \to \nu_e$ and $\nu_\mu \to \nu_\tau$ and expected sensitivity of future experiments (dotted lines).

or by neutral-current interaction

$$\begin{aligned} \nu_i &\rightarrow e + \text{hadrons} \\ \nu_i &\rightarrow \mu + \text{hadrons} \end{aligned} \tag{14}$$

The charged-current coupling of massive neutrinos ν_i to a charged lepton ℓ is proportional to $|U_{\ell i}|^2$, where $U_{\ell i}$ are elements of the mixing matrix (eq.(5)). The lifetime can be related to the muon lifetime τ_μ according to the following expression

$$\tau_{\nu_i} = \tau_{\nu_\mu} (m_\mu/m_{\nu_i})^5/|U_{\ell i}|^2 \tag{15}$$

for a neutrino mass equal to the muon mass the lifetime is increased by the factor $|U_{\ell i}|^{-2}$.

The decay rate over a distance L is proportional to $m_{\nu_i}^{\ 6}$

$$\text{Rate } (\nu_i \rightarrow \ell_1 \ell_2 \nu_{\ell_2}) \propto |U_{\ell i}|^2 \, m_{\nu_i}^{\ 6} \cdot L/E_{\nu_i} \ . \tag{16}$$

The same dependence on $U_{\ell i}$ has been assumed for neutral-current interactions, the possibility of flavour changing contributions was deliberately neglected.

Heavy neutrinos can be produced either in the decays of pions and kaons or, for larger masses exceeding the pion and kaon mass, in the decay of heavy mesons, for instance D mesons.

The principle of the laboratory searches [42] for neutrino decays is illustrated in figure 19. High energy protons incident on a target produce mesons which decay into a charged lepton (ℓ = e,μ) and a neutrino which can mix with a heavy neutrino ν_i This neutrino may decay, according to one of the modes given in eqs. (13,14). The mixing parameter $U_{\ell i}$ occurs in both processes, in that of meson decay and in the neutrino decay and the number of decay events is therefore proportional to $|U_{\ell i}|^4$.

A dedicated detector of low density to minimize neutrino interactions has been built by the CHARM Collaboration [42] to search for neutrino decays in conventional neutrino beams and in beam dump experiments. Later a similar detector was also exposed in a low energy neutrino beam to enhance the rate [43].

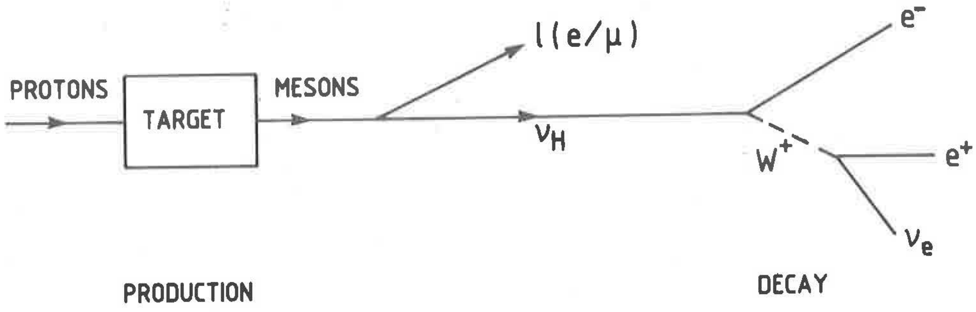

Fig. 19 Search for decays of heavy neutrinos [42]. The mixing parameters appear in meson decay and in ν_H decay.

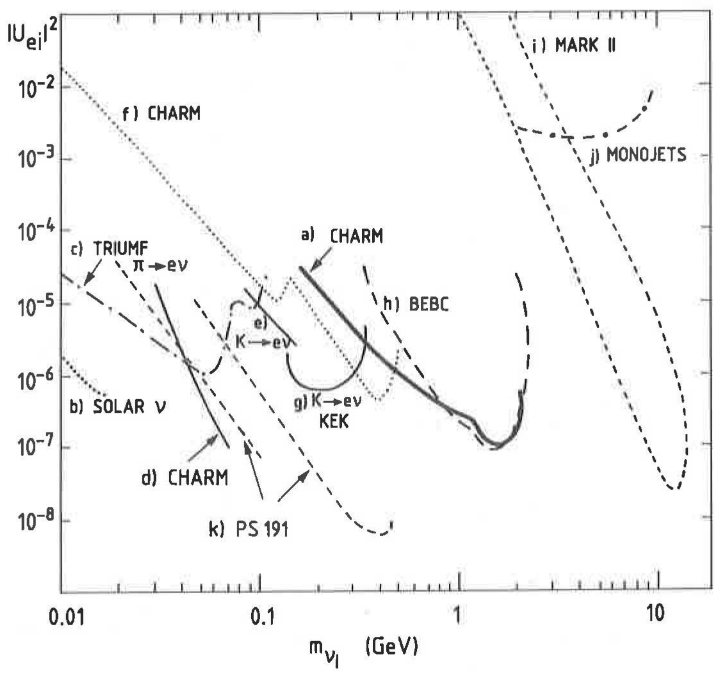

Fig. 20 Summary of 90% c.l. limits on $|U_{ei}|^2$. The area above the curves is excluded.

These detectors have a length of ~ 40 m; however, as they are traversed by about 10^{14} neutrinos, the experiments are sensitive to decay lengths of the order of 10^{16} m, which are also significant for astrophysics. No decay has been identified. The limits on $|U_{ei}|^2$ and $|U_{\mu i}|^2$ are shown in figures 20 and 21 respectively. They extend to mass values of 2 GeV; for masses between 100 and 400 MeV these limits are 10^{-7} to 10^{-8}, corresponding to lifetimes of the order of 10 sec. This search will be extended to higher mass values at the large e^+e^- colliders SLC and LEP using the production process

$$Z^0 \rightarrow \nu_i \bar{\nu}_i \ . \tag{17}$$

For $m_{\nu_i} = 40$ GeV and $|U_{\ell i}|^2 = 10^{-4}$ the corresponding lifetime would be $10^{-9} \cdot \tau_\mu$.

3.3 The Solar Neutrino Puzzle

The sun is an intense source of electron neutrinos, produced in the proton-proton chain and in the CNO cycle (see table 4 and figure 22); the flux incident on the earth is ~ 10^{11} $\nu_e/cm^2 \cdot s$. The flux and the energy distribution of these neutrinos carry important information about the thermonuclear reactions which take place in the core of the sun. For our knowledge of stellar evolution solar neutrinos are therefore a unique source of information. For particle physics these solar neutrinos are of the greatest importance, because of the distance of 10^{11} m they have travelled to the earth and the corresponding ratio L/E ~ 10^{10}-10^{11} m/MeV, they provide sensitivity to neutrino oscillations with mass differences of $\Delta m^2 \sim 10^{-11}$ eV^2. Exploiting the small seasonal modulation of the distance earth-sun of about 3% would even increase that sensitivity to $\Delta m^2 \sim 10^{-12}$ eV^2 [44]. For a recent review of both aspects see W.C. Haxton's and Hampel's reports at the 1984 Neutrino Conference [45].

The experimental goal in solar neutrino physics is to determine the pp, ^{7}Be and ^{8}B neutrino fluxes separately in order to get information on the relative rates of the different cycles of thermonuclear reactions which produce them, and to vary L/E in search for neutrino oscillations. This program was started by R. Davis Jr. in 1970 by measuring the capture rate of the reaction

$$\nu_e + {}^{37}Cl \rightarrow e^- + {}^{37}Ar \tag{18}$$

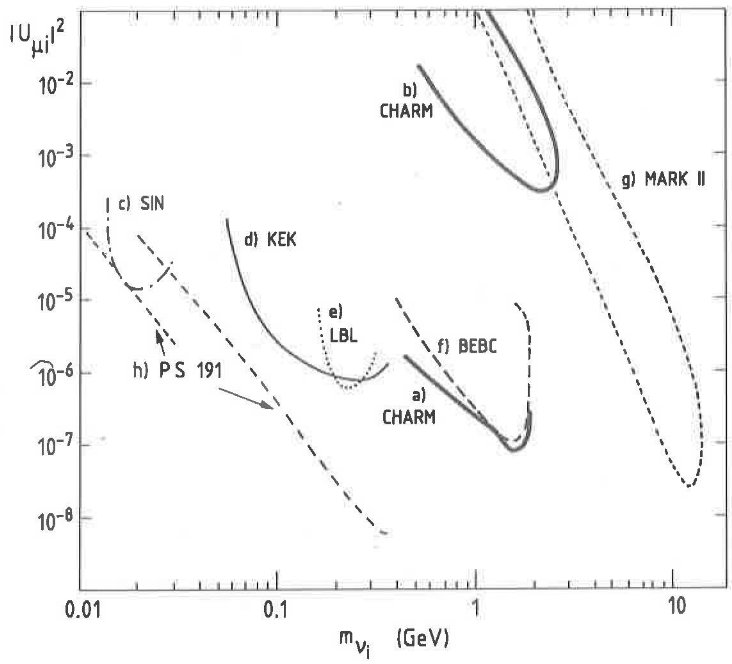

Fig. 21 Summary of 90% c.l. limits on $|U_{\mu i}|^2$.

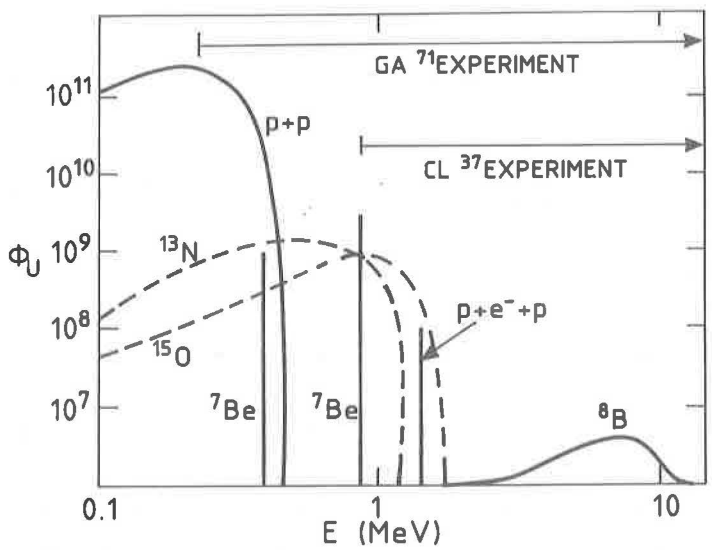

Fig. 22 Energy spectrum of the flux of the different components of solar neutrinos.

Table 4

Summary of reactions producing neutrinos in the pp chain and CNO cycle

Source	E_ν(max) MeV	Flux ($10^{10}/cm^2 \cdot s$)	Event rate in SNU	
			^{37}Cl	^{71}Ga
$p+p \to {}^2H+e^+ + \nu_e$	0.42	6.1	–	71.3
${}^{13}N \to {}^{13}C+e^+ + \nu_e$	1.20	$5 \cdot 10^{-2}$	0.08	2.9
${}^{15}O \to {}^{15}N+e^+ + \nu_e$	1.73	$4 \cdot 10^{-2}$	0.26	4.0
${}^{8}B \to {}^{8}Be+e^+ + \nu_e$	14.06	$5.6 \cdot 10^{-4}$	5.28	1.4
${}^{7}Be+e^- \to {}^{7}Li+\nu_e$	0.86 (90%) 0.38 (10%)	$4.3 \cdot 10^{-1}$	1.09	31.2
$p+e^- + p \to {}^2H+\gamma$	1.44	$1.5 \cdot 10^{-2}$	0.23	2.5
Sum		$6.64 \cdot 10^{10}$	6.9 SNU	113 SNU

in the Homestake Gold Mine, South Dakota, using a tank filled with 615 tons of perchlorethylene. He performed [46], from 1970 to 1983 many data runs and purged the liquid each time with helium gas to remove ^{37} Ar atoms produced in reaction (18). These atoms are then counted by means of their electron capture radioactivity ($T_{1/2}$ = 35d). The result of 59 runs is (see figure 23)

$$0.47 \pm 0.04 \ {}^{37}\text{Ar atoms/day}$$

of which 0.08 ± 0.03 are attributed to cosmic ray background, yielding a capture rate of

$$R_{exp}({}^{37}Cl) = 2.1 \pm 0.3 \ \text{SNU} . \qquad (19)$$

(1 SNU = 10^{-36} captures/^{37} (1 atom · s)

The standard model of the sun predicts [47] for this rate

$$R_{th}\ ({}^{37}Cl) = 7.6 \pm 1.5 \ \text{SNU} , \qquad (20)$$

Table 4 gives the contributions of the different sources. Restricting the discussion to the high energy neutrinos from ^{8}B, the Davis experiment requires a strong reduction of this flux and is consistent with a total absence of these high energy neutrinos.

What is the explanation of this solar neutrino puzzle?

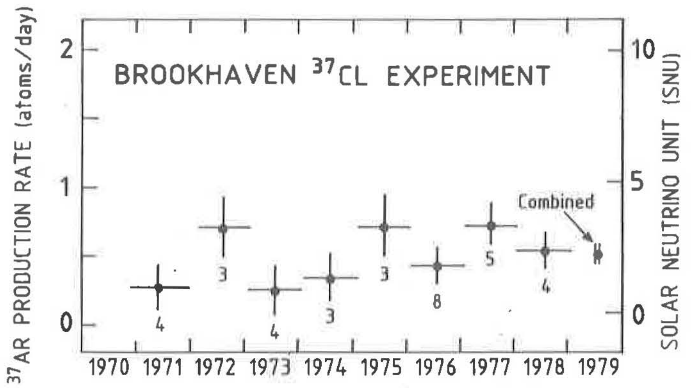

Fig. 23 Capture rate of solar neutrinos in ^{37}Cl observed by Davis.

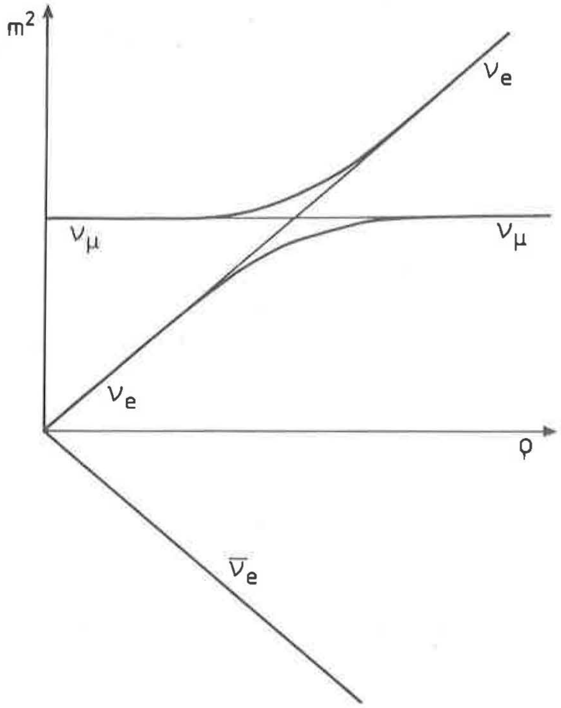

Fig. 24 Neutrino mass as a function of electron density in the sun, following Bethe [50].

Experimental uncertainties can be ruled out. Davis has demonstrated that ^{37}Ar, artificially produced in the tank, is recovered with full efficiency. The capture cross section for ^{8}B neutrinos has been measured on ^{37}Cl using small angle (p,n) reactions.

The model of the solar core may be questioned [47]. This is touching on far-reaching implications for the theory of stellar evolution. Recent measurements of solar oscillations can probe the solar core in an independent way.

The sun may burn as expected but the electron neutrino state may be modified during its transit through the sun or its travel to the earth. The full program of solar neutrino spectroscopy has to be carried out to distinguish between these possibilities.

The Davis result may arise if the neutrino is a four-component Dirac particle with a magnetic moment μ [48]. Propagating through the magnetic field of the solar convective zone the neutrino helicity would be partly reversed, thus decreasing the flux of left-handed neutrinos detected in the experiment. The resulting right-handed neutrinos are sterile in the Davis experiment.

After propagation through a magnetic field H, with a component $H_\perp$ perpendicular to the direction of the neutrino motion, the following numbers of left-handed and right-handed neutrinos appear:

$$N_L = N_\nu \cos^2 (\mu HL)$$
$$N_R = N_\nu \sin^2 (\mu HL) \qquad (21)$$

where $HL = \int H_\perp dl$, and L is the thickness of the convective zone. According to estimates [48] $L \simeq 2 \cdot 10^{10}$ cm and $H \simeq (1\text{-}5)10^3$ Gauss. If $\mu \sim (0.3\text{-}1)10^{-10}\ \mu_B$, ($\mu_B$) is the Bohr magneton, the product μHL may reach the value $\pi/4$, corresponding to a factor 2 suppression of N_L (see eq.(21)). The required value of the magnetic moment is not excluded by present experimental limits (see Chapter IV). To prove this explanation, the 11 year solar cycle which modulates the magnetic field would have to be observed, independent of the energy of neutrinos.

A new explanation in terms of neutrino oscillations has recently been proposed by Mikheyev and Smirnov [49] and by H. Bethe [50]. Neutrino oscillations had already been invoked much earlier [44], but required then maximum mixing of three neutrino states, whereas small mixing angles of the order of $(m_e/m_\mu)^{1/2}$ or $(m_\mu/m_\tau)^{1/2}$ are expected theoretically. The new explanation takes into account, as pointed out by Wolfenstein in 1978 [51], that in matter neutrino masses are changed due to the weak-current interaction. While the interaction between ν_e and electrons is due to both the neutral and the charged current, the scattering of ν_μ on electrons is due to the neutral current alone. The additional W exchange term is equivalent to a potential energy for ν_e of

$$V = G_F \sqrt{2} \ N_e ,$$

where G_F if the Fermi constant of weak interactions and N_e is the number of electrons per cm³. This potential V adds a term to $m_\nu{}^2$ of

$$m_i{}^2 = 2E_\nu V = 2 \sqrt{2} G_F N_e E_\nu = \rho . \quad (22)$$

Figure 24 shows the two eigenvalues of $m_\nu{}^2$ as a function of the electron density ρ. At low ρ, the electron neutrino has the smaller mass, but when ρ approaches the value

$$\rho = (m_2{}^2 - m_1{}^2)\cos 2\theta \quad (23)$$

the two curves almost cross. The minimum distance or mass splitting is given by the term $(m_2{}^2-m_1{}^2)\sin 2\theta$. At larger ρ, beyond the crossing point, the electron neutrino has larger mass than the muon neutrino. At the crossing point the effective mixing angle goes through a resonance and becomes $\pi/4$. An electron neutrino, produced at high ρ in the core of the sun and propagating towards the surface (small ρ), will come to the resonance and will then continue to follow the upper mass curve and will therefore emerge from the sun as a muon neutrino, which is inactive in the Davis experiment.

Let us assume now the Davis' experiment detected electron neutrinos with $E < E_{critical}$, which do not go through the resonance, with full flux, whereas all other neutrinos with $E > E_c$ are converted into ν_μ. Based on this assumption Bethe [50] estimated

$$\Delta m^2 \cos 2\theta = 4.5 \cdot 10^{-5} \ eV^2 . \quad (24)$$

The rate of neutrino capture in Gallium

$$\nu_e + {}^{71}Ga \rightarrow e^- + {}^{71}Ge \quad (25)$$

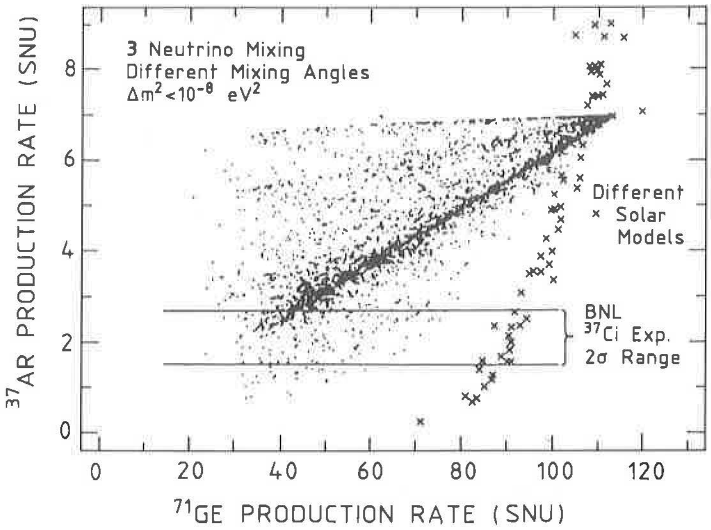

Fig. 25 Relation of the solar neutrino capture rate in ^{37}Cl and in ^{71}Ga for different solar models and neutrino mixing parameters (following Hampel [45]).

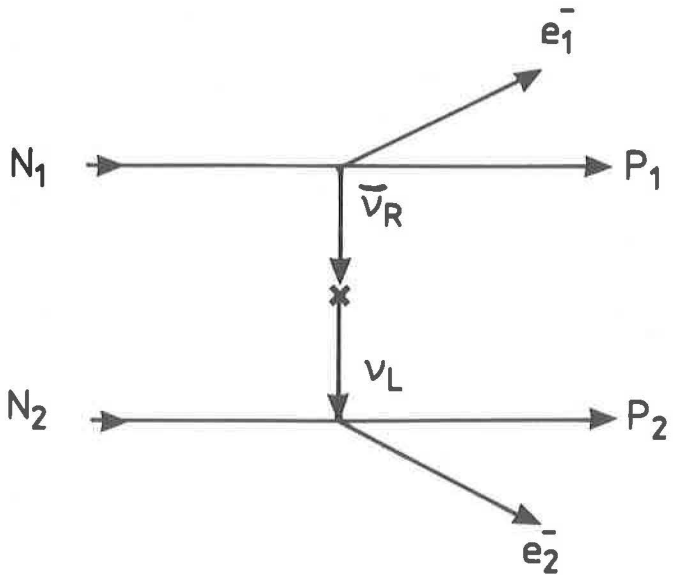

Fig. 26 Neutrinoless double beta-decay. At the cross a transition from $\bar{\nu}_R$ to ν_L has to occur, requiring a massive Majorana neutrino.

(see table 4) would be very little modified if this explanation is valid; the total rate of 113 SNU would be reduced by 1.4 SNU. Observation of solar neutrinos by a Ga detector would therefore confirm or invalidate this theory.

With $\Delta m^2 = 4.5 \cdot 10^{-5}\ eV^2$, assuming $\cos 2\theta = 1$ in eq. (24), confirmation in laboratory experiments is extremely difficult. At a nuclear reactor (3 GW) a distance to the detector of 100 km is required. Present detectors with an active target of 0.3 ton would have to be scaled up to 10^6 tons.

A Ga detector [45] (Gallex Collaboration) of 30 tons, to be situated in the Gran Sasso tunnel in Italy, is under construction and will start data taking in 1990. The capture rate will be measured with a statistial error of 5%. Figure 25 shows how this experiment can discriminate between different solar models and neutrino oscillations.

3.4 Neutrinoless Double Beta Decay

The observation of neutrinoless double beta decay would be a dramatic discovery as it implies the existence of massive Majorana neutrinos. The corresponding Feynman diagram is shown in figure 26. This process is energetically possible as the pairing energy in nuclei with even numbers of neutrons and protons provides stronger binding than in neighbouring odd-odd nuclei. The even-even nucleus cannot, therefore, decay to the neighbouring odd-odd nucleus, because of the energy balance, but the decay to the next even-even nucleus is energetically allowed via second order weak interaction. The $\bar{\nu}_R$ emitted in the decay of N_1 (figure 26) has to be captured by N_2 as a state ν_L. Hence, the neutrino must be a Majorana state, to ensure no distinction between ν an $\bar{\nu}$ states is possible, and massive to allow a flip of the helicity from right-handedness to left-handedness. The amplitude, involving helicity flip, is proportional to m_ν. A small amplitude of the "wrong" helicity state can also be induced by right-handed weak currents. However, these currents are strongly suppressed, by the GIM mechanism and by the intrinsic weakness of these currents owing to the large mass of the corresponding right-handed intermediate boson. I shall therefore restrict the discussion to the more favoured $0^+ \rightarrow 0^+$ transition to the ground state induced by massive Majorana neutrinos.

Several groups have reported on an experimental search for neutrinoless double beta decay of ^{76}Ge [52-57]. The present best lifetime limits are summarized in Table 5. Natural germanium contains 7.76% of ^{76}Ge and is itself a precise electron detector. The 0^+-0^+ transition would give a peak in the beta spectrum at the sum of the two electron energies $E_1+E_2 = 2040.71 \pm 0.52$ keV, with a full width of ~ 3 keV. The sensitivity of the experiment depends on the quantity of active germanium and on the background level at $E \simeq 2$ MeV. Backgrounds come from cosmic rays (secondary neutrons) and from radioactivity of the other materials of the detector. Special measures have been taken to reduce the background caused by radioactivity in the cryostat walls. Reduction of cosmic ray background was achieved by active shielding around the germanium detectors and by passive shielding in underground laboratories. The Milano experiment is located in the Mont Blanc tunnel under ~ 3000 m of rock.

Table 5
Summary of limits on neutrinoless double beta decay

Group	Detector	Background (counts per KeV.hr. (100^3cm))	Lifetime limit (68% c.l.)
Milano [52]	116 cm^3Ge	$1.4 \cdot 10^{-3}$	$6.9 \cdot 10^{22}$y
	143 cm^3Ge	$0.24 \cdot 10^{-3}$	$1.7 \cdot 10^{23}$y
UCSB/LBL [53]	2 x 160 cm^3Ge	$0.76 \cdot 10^{-3}$	$3.6 \cdot 10^{22}$y
	8 x 160 cm^3Ge		$1.2 \cdot 10^{23}$y
Guelph/Aptec/ Kingston [54]	600 cm^3Ge	–	$1.2 \cdot 10^{23}$y
Osaka [55]	160 cm^3Ge	$1.6 \cdot 10^{-3}$	$2.2 \cdot 10^{22}$y
Cal Tech [56]	90 cm^3Ge	$1.8 \cdot 10^{-3}$	$2.0 \cdot 10^{22}$y
	1000 cm^3Ge	under construction	
Batelle/South Carolina [57]	125 cm^3Ge	$0.2 \cdot 10^{-3}$	$1.3 \cdot 10^{22}$y

No experiment has up to now observed neutrinoless double beta decay. What can be learned from the lifetime limits? Can a limit on m_ν be extracted? To attempt this we have to calculate with confidence the nuclear part of the matrix element. These calculations have been checked on $(\beta\beta)2\nu$ decays and tend to give lifetimes which are an order of magnitude too short. A recent calculation by K. Grote and H.V. Klapdor [58] gives a mass limit of

$$\langle m_\nu \rangle < 1.6 \text{ eV} . \tag{26}$$

The true electron neutrino mass might, however, be substantially larger than this limit. If neutrinos of different flavour or light and heavy neutrinos of the same flavour contribute to the matrix element they can interfere destructively, because of different CP parities [59]. Owing to these cancellations it is possible to have even the extreme situation in which massive Majorana neutrino states do exist but the effective mass in neutrinoless double beta decay is zero.

It seems therefore to be important to note that non-observation of $(\beta\beta)0_\nu$ decay does not imply $m_\nu = 0$ or the absence of Majorana neutrino fields in nature.

4. ELECTROMAGNETIC PROPERTIES OF NEUTRINOS

The questions of electric neutrality of neutrinos, of a finite electric charge radius and of a magnetic moment and their effects in passage through matter, have been debated ever since Pauli postulated the existence of neutrinos.

Carlson and Oppenheimer [60] derived in 1932 the ionization loss of neutrinos in interactions with electrons and found in lowest order a logarithmic increase with energy, later corrected by Bethe [61]. They concluded that neutrinos would not make a visible track in cloud chambers. The discussion about the magnetic moment of neutrinos was started by Pauli in his article in the Handbuch der Physik in 1933 [62] where he recognized that neutrinos might have an anomalous (Pauli) moment. Later Houtermans and Thirring [63], Bernstein et al. [64], M.Goldhaber [65] and Barut [66] made contributions to calculate the magnetic moment (μ).

Today we know that if the neutrino mass is zero and there is a two-component neutrino, μ must be zero, because a non-zero magnetic moment would introduce spin flips and, hence, four neutrino components. If neutrinos were massive Dirac particles they will have undoubtedly an induced magnetic moment which differs from zero. In the Glashow-Weinberg-Salam standard model we have in this case [67]

$$\mu^{st} = \frac{3eG_F}{8\sqrt{2}\pi^2} m_\nu = 3.2 \cdot 10^{-19} \mu_B \left(\frac{m_\nu}{1\ \mathrm{eV}}\right) \qquad (27)$$

where μ_B is the electron Bohr magneton. Much larger values of μ are possible in left-right symmetric theories and in theories with non-standard Dirac neutrinos [67], with values exceeding μ^{st} by 4 to 5 orders of magnitude.

The best experimental limits on the electromagnetic properties of neutrinos are derived from experiments on neutrino scattering from electrons. Cowan and Reines [68] concluded from measurements of $\bar{\nu}_e e$ scattering in a nuclear reactor experiment

$$\mu_{\nu_e} < 1.4 \cdot 10^{-9}\ \mu_B \text{ (95\% c.l.)} \tag{28}$$

The CHARM Collaboration [69] at CERN determined from measurements of $\nu_\mu e$ and $\bar{\nu}_\mu e$ scattering with a mean energy of 20 GeV limits on the magnetic moment

$$\mu_{\nu_\mu} < 1.5 \cdot 10^{-8}\ \mu_B \text{ (95\% c.l.)} , \tag{29}$$

on the electric charge

$$Q_{\nu_\mu} < 10^{-10} e \text{ (95\% c.l.)} , \tag{30}$$

and on the electric charge radius defined by $F(q^2) \cong {}^1/_6 \langle r_Q{}^2 \rangle q^2$

$$\langle r_Q{}^2 \rangle^{1/2} < 10^{-16} \text{ cm} . \tag{31}$$

Future high statistics experiments will further improve these limits. The possible role of a non-zero magnetic dipole moment for the explanation of the solar neutrino puzzle was discussed in Chapter III.3.

5. CONCLUSIONS AND OUTLOOK

The present experimental situation can apparently be best described by massless, perfectly neutral neutrinos, created with three or at the most 2.4 additional flavours and conserving them.

Three of the claimed manifestations of finite neutrino mass have been contradicted. In the case of the ITEP finite mass claim the analysis by Bergkvist implies the rejection of the experimental evidence, and the new result of Kündig's group in Zürich excludes the magnitude of the neutrino mass claimed. The case of the 17 keV neutrino claim can also be considered as rejected by the results of new experiments, despite apparent flaws in the analysis of three of them. The objections raised against the indications of neutrino oscillations in the Bugey experiment clearly weaken that case and do , in my judgement, invalidate this claim.

It will be very interesting to see the results of the extended Bugey experiment, using two detectors with greatly improved neutron detection efficiencies simultaneously.

Very refined new measurements of the end point of the tritium beta decay spectrum are being planned or are under way. If the electron neutrino mass is not smaller than 10 eV it should be possible to establish that it is non-zero in an unambiguous way within the next years.

The notion that the flavour of a neutrino is uniquely related to the flavour of the associated charged lepton may be too narrow to allow a precise description of all neutrino phenomena, but up to now no compelling evidence for neutrino mixing, in oscillations or decays, has been found in laboratory experiments. A fascinating new explanation of the solar neutrino puzzle has recently been put forward, based on resonance amplification of neutrino mixing in dense matter. The Gallium solar neutrino detector which is presently under construction, will be able to discriminate amongst the different explanations of the solar neutrino puzzle. It provides particle physics with the fascinating possibility of searching for neutrino mixing with $\Delta m^2 \sim 10^{-12}$ eV^2. Future searches for neutrino oscillations at accelerators which are now being proposed can extend the sensitivity to small mixing angles, of $|U_{\mu e}|^2$ and $|U_{\mu\tau}|^2 \sim 10^{-3}$ for $\Delta m^2 \sim 1$ eV^2. Searches at nuclear reactors, using more sophisticated detectors at larger distances, will extend the sensitivity to $\Delta m^2 \sim 10^{-3}$ eV^2 for larger values of the mixing parameter.

The question of distinguishing between massive Dirac and Majorana neutrino is still open, and can only find an answer by the discovery of neutrinoless double beta decay. Here we can expect new results extending the lifetime sensitivity for $^{76}Ge \rightarrow {}^{76}Se + 2e^-$ decays to 10^{24} y. Different nuclei are also being investigated (e.g. $^{136}Xe \rightarrow {}^{136}Ba$), because the possibility of cancellations in the nuclear matrix element of ^{76}Ge decays cannot be completely excluded.

Still further away in the future, there may one day be the possibility of detecting the cosmic relic neutrinos.

These open questions will be a lasting challenge in experimental particle physics.

REFERENCES

1. W. Pauli, letter to the "Radioactive ladies and gentlemen", see e.g. L.M. Brown in Physics Today, Sept. 1978, p.23.

2. J. Chadwick, Z.f. Physik 31 (1914) 210
   C.D. Ellis, W.A. Wooster, Proc. Roy. Soc. (London) A117 (1927) 109
   L. Meitner, W. Orthmann, Z.f. Physik 60 (1930) 143.

3. E. Fermi, Z.f. Physik 88 (1934) 161.

4. F. Perrin, Compt. Rend. 197 (1933) 1625.

5. See e.g. Ken-ichi Hikasa, preprint MAD/PH/269, Univ. Wisconsin, Madison Nov. 1985.

6. D.N. Schramm in Tenth Texas Symposium on Relativistic Astrophysics, Baltimore 1981.

7. J. Yang, M.S. Turner, G. Steigman, D.N. Schramm and K.A. Olive, Ap.J. 281 (1984) 493.

8. J. Ellis, K. Enqvist, D.V. Nanopoulos and S. Sarkar, Phys. Lett. 167B (1986) 457.

9. L. Di Lella, Proc. of 1985 Int. Symposium on Lepton and Photon Interactions (Kyoto, Japan 1985) p.280.

10. See e.g. Physics at LEP, CERN 86-2, Vol. 1, pp. 47 and 197 (edited by J. Ellis and R. Peccei).

11. See e.g. B. Kayser, Proc. of 4th Moriond Workshop on Heavy Neutrinos in Particle and Astrophysics (1984).

12. B. Kayser, Phys. Rev. 26 (1982) 1662.

13. K. Winter, Phys. Lett. 67B (1977) 236.

14. K. Bergkvist, Proc. Int. Symposium Lepton and Photon Interactions (Kyoto, Japan, 1985) p. 560.

15. V.A. Lubimov et al., Phys. Lett. 94B (1980) 266.
S. Boris et al., Proc. Int. Europhysics Conf. on High Energy Physics (Brighton, UK, 1983) p. 386.
S. Boris et al., Proc. 22nd Int. Conf. High Energy Physics (Leipzig, DDR, 1984) Vol. 1, p.257.
S. Boris et al., Phys. Lett. 159B (1985) 217
V.A. Lubimov at 6th Moriond Workshop on Massive Neutrinos in Particle and Astrophysics (1986).

16. J.J. Simpson, Phys. Rev. Lett. 54 (1985) 1891.

17. B. Jackelmann et al., Phys. Rev. Lett. 56 (1986) 1444 and
R. Abela et al., Phys. Lett. 146B (1984) 431.

18. ARGUS Collaboration, Proc. VIth Moriond Workshop on Massive Neutrinos in Particle Physics and Astrophysics (Tignes, France, 1986).

19. K.E. Bergkvist, Nucl. Phys. B39 (1972) 317.

20. E.F. Tretyakov, Izv. Akad. Nauk SSSR Ser. Fiz. 39 (1975) 583.

21. J.J. Simpson, Phys. Rev. D30 (1984) 1110.

22. K.E. Bergkvist, Phys. Lett. 154B (1985) 224 and Phys. Lett. 159B (1985) 408.

23. M. Fritschi, E. Holzschuh, W. Kündig, J.W. Petersen, R.E. Pixley and H. Stüssi, Phys. Lett. B, in print.

24. A. Apalikov et al., preprint ITEP-114 (1985).

25. T. Ohi et al., Phys. Lett. 160B (1985) 322.

26. V.M. Datar et al., Nature 318 (1985) 547.

27. T. Altzitzoglov et al., Phys. Rev. Lett. 55 (1985) 799.

28. J. Markey and F. Boehm, Phys. Rev. C32 (1985) 2215.

29. J.J. Simpson, Proc. VIth Moriond Workshop on Massive Neutrinos in Particle Physics and Astrophysics (Tignes, France, 1986).

30. J. Lindhard and P.G. Hansen, preprint Univ. Aarhus, Denmark, March 1986.

31. H. Blümer, K. Kleinknecht, Phys. Lett. 161B (1985) 407.

32. J.L. Vuilleumier et al., Phys. Lett. 114B (1982) 298.

33. Caltech-SIN-TUM Collaboration,
Gabathuler et al., Phys. Lett. 138B (1984) 449
Zacek et al., Z.f. Physik (in print) and Phys. Lett. 164B (1985) 193.
R. Mössbauer, Proc. First ESO-CERN Symposium, CERN, Geneva 1983, (G. Setti, L. Van Hove, ed.) p. 273.

34. J.F. Cavaignac et al., Phys. Lett. 148B (1984) 387.

35. H. Sobel et al., (private communication).

36. A.I. Afonin et al., JETP Lett. 42 (1985) 285.

37. L.A. Ahrens et al., Phys. Rev. D31 (1985) 2732.

38. BEBC Collaboration, see J. Wotschack, Proc. 11th Conf. on Neutrino Physics, Nordkirchen, FRG (1984) p. 177.

39. N.J. Baker et al., Phys. Rev. Lett. 47 (1981) 1576.

40. F. Bergsma et al., CHARM Collab., Phys. Lett. 142B (1984) 217.

41. R.E. Shrock, Phys. Rev. D24 (1981) 1232
M. Gronau, Phys. Rev. D28 (1983) 2762.

42. F. Bergsma et al., CHARM Collab., Phys. Lett. 128B (1983) 361, and Phys. Lett 166B (1986) 473.

43. G. Bernardi et al., Phys. Lett. 166B (1986) 479.

44. S.M. Bilenky and B. Pontecorvo, Phys. Rep. 41C (1978) 255.

45. W.C. Haxton, Proc. 11th Conf. on Neutrino Physics, Nordkirchen, FRG, 1984, p.214.
W. Hampel, idem, p.530.

46. R. Davis Jr., Proc. Neutrino Mass Miniconf. Telemark, Wisconsin (1980), ed. V. Barger and D. Cline, p.38.

47. J.N. Bahcall et al., Rev. Mod. Phys. 54 (1982) 767.

48. E.G. Gibson, "The Quiet Sun", NASA, Washington 1973,
L.B. Okun, M.B. Volashin, M.I. Vysotsky, ITEP preprint 1986-20, Moscow 1986,
A. Cisneros, Astrophys. Space Sci., 10 (1971) 87.

49. S.P. Mikheyev and A. Smirnov, 10th International Workshop on Weak Interactions, Savonlinna, Finland, June 1985.

50. H.A. Bethe, Phys. Rev. Lett. 56 (1986) 1305.

51. L. Wolfenstein, Phys. Rev. D17 (1978) 2369.

52. E. Fiorini et al., Nuovo Cim. 13A (1973) 747,
E. Bellotti et al., Phys. Lett. 121B (1983) 72.

53. D. Caldwell et al., Proc. of XXIIth Int. Conf. on High Energy Physics, Leipzig 1984, Vol.1, p.270, and in ref. [14].

54. J.J. Simpson, P. Jagam, J.L. Campbell, H.L. Malm and B.C. Robertson, Phys. Rev. Lett. 53 (1984) 141.

55. H. Ejiri, N. Takahashi, T. Shibata, Y. Nagai, K. Okada, S. Nakayama and N. Kamikubota, Osaka University preprint.

56. A. Forster, H. Kwon, J.K. Markey, F. Boehm and H.E. Henrickson, Phys. Lett. 138B (1984) 146.

57. F.T. Avignone, R.L. Brodzinski, D.P. Brown, J.C. Evans, W.K. Hansley, J.H. Reeves and N.A. Wogman, Phys. Rev. Lett. 50 (1983) 721.

58. K. Grote, H.V. Klapdor, paper presented at 1st Symposium on Underground Physics, Saint Vincent, Italy, April 1985.

59. W.C. Haxton and G.C. Stephenson, "Double beta decay" Progress in Particle and Nucl. Physics, 12 (1985) 409.
See also T. Kirsten in Proc. 11th Int. Conf. Neutrino Physics, 1984, p.145, and E. Bellotti, idem, p.171.

60. C. Carlson, R. Oppenheimer, Phys.Rev. 41 (1932) 763.

61. H.A. Bethe, Proc. Cambr. Phil. Soc. 31 (1935) 108.

62. W. Pauli, Handbuch der Physik 1933, Vol. 24/1 p.233.

63. F.G. Houtermans, W. Thirring, Helv. Physica Acta 27 (1954) 81.

64. J. Bernstein, G. Feinberg, M. Ruderman, Phys. Rev. 132 (1963) 1227.

65. M. Goldhaber, Proc. Int. Neutrino Conference 1974 (Philadelphia) ed. C. Baltay.

66. A.O. Barut, Proc. Neutrino Mass Mini Conf. Telemark, Wisconsin 1980 (ed. V. Barger, P. Cline) p.130.

67. A.V. Kyuldjiev, Nucl. Phys. B243 (1984) 387 and references therein.

68. C. Cowan, F. Reines, Phys. Rev. 107 (1975) 528.

69. CHARM Collaboration (to be published) see also PhD thesis of Th.Hebbeker, Univ. Hamburg 1986.